

Thermoelectric Properties of Texture-controlled MnSi_{1.7}-based Composite Thin Films

Yosuke Kurosaki*, S. Yabuuchi, A. Nishide, N. Fukatani and J. Hayakawa

Center for Exploratory Research, Research & Development Group, Hitachi, Ltd., 1-280, Higashi-koigakubo, Kokubunji, Tokyo 185-8601, Japan

Abstract

Thermoelectric properties of composite thin films with higher manganese silicide (MnSi_{1.7}) and silicon (Si) were investigated together with textures and crystal structures. The MnSi_{1.7}-based thin films were fabricated from multilayers of manganese and silicon by post annealing using planar coupling reactions in the interfaces between the manganese and silicon layers. Moreover, to improve the morphology of the films, the layer thicknesses were changed. As a consequence, smooth and voidless thin films consisting of crystallized MnSi_{1.7} were successfully obtained by solid-phase reactions when the thickness of the manganese layer was less than 2 nm. The resistivity of the thin films was reduced about 30% by decreasing the initial manganese thickness when the Si/Mn composition ratio was 2.1. In addition, the Seebeck coefficient was increased to 225 $\mu\text{V/K}$ at 390°C, which is close to the maximum in MnSi_{1.7}-based compounds, by controlling annealing temperature and annealing time.

Publication History:

Received: November 04, 2016

Accepted: January 11, 2017

Published: January 13, 2017

Keywords:

Thermoelectric properties, MnSi_{1.7}, Fermi energy, Morphology

Introduction

As a means for recovering a vast amount of waste heat, thermoelectric devices have been attracting a lot of interest. Although a wide variety of thermoelectric materials exist, candidates are still limited because of the strict demands for not only high thermoelectric performance but also nontoxicity, abundance, and inexpensiveness. The material thermoelectric performance is generally evaluated by a dimensionless figure of merit ZT, which is given by $S^2T/\rho\kappa$, where S is Seebeck coefficient, ρ is electrical resistivity, T is absolute temperature, and κ is thermal conductivity. As a potential material for satisfying the above demands with ZT over 1.0, higher manganese silicide (MnSi_{1.7}), which is known to be semiconducting, has been focused on [1]. The crystal structure of MnSi_{1.7} is known as Nowotny chimney ladder phase, in which a manganese (Mn) sublattice forms a chimney like structure, while silicon (Si) exists in a helical fashion [2,3]. MnSi_{1.7} has an energy gap of 0.7-0.8 eV, and the large density of states near the Fermi energy contributes to large S [4,5]. The power factor (S^2/ρ) exceeds 2×10^{-3} W/Km, while κ is low ranging from 2.0 to 3.0 W/Km owing to its complex crystal structure [2,3]. For further improvements in ZT, nanocomposite structures are known to be effective [6,7] and are relatively easy to be realized in thin films compared with bulk forms. In the author's previous study, in which nanometer-scale MnSi_{1.7}/Si multilayers were fabricated by controlled thermal diffusions of Mn and Si atoms, κ was successfully reduced to 1.0 W/Km, which is the experimentally observed minimum in MnSi_{1.7}-related materials [8]. Recently, the importance of planar binary coupling reactions at the interface between transition metals and Si has been recognized for the formation of transition metal silicide thin films [9-11]. To modulate the texture and improve the thermoelectric properties of MnSi_{1.7}-based composite thin films, planar Mn-Si coupling reactions should be investigated in detail and should be controlled.

In this study, we focused on planar Mn-Si coupling reactions and investigated changes of thermoelectric properties with the textures and crystal structures of MnSi_{1.7}-based thin films. We fabricated MnSi_{1.7}-based thin films by annealing multi-layered thin films in which Mn and Si layers were deposited alternately. To examine the nature of coupling reactions between Mn and Si in the post-annealing process, we first investigated dependence of crystal structures of annealed Mn/Si bi-layered thin films and their thermoelectric properties on the

composition ratio between Mn and Si. Next, we also evaluated the morphology of the fabricated MnSi_{1.7} thin film. After that, we tried to improve the morphology of MnSi_{1.7} thin films by reducing the initial thickness of Mn and Si layers since planar coupling reactions are considered to occur only in the vicinity of interfaces between Mn and Si layers. Then, for evaluating S of the thin films in high-temperature regions, we measured S of MnSi_{1.7} thin films on a thermally oxidized Si substrate and we clarified that the substrate is inappropriate for measuring S even if it is insulated with SiO_x layers. Finally, we investigated an effect of post annealing on crystal structures and thermoelectric properties of MnSi_{1.7}-based composite thin films with Si fabricated on sapphire substrates.

Experimental Procedure

Samples were prepared as follows. Multilayers (MLs) of Mn and Si were deposited by magnetron sputtering techniques with a base pressure of 10^{-6} Pa at room temperature (RT) on thermally oxidized Si substrates, in which the thickness of SiO_x was 700 nm, and sapphire substrates. Hereafter, SiO_x//, Sapp//, and MLs (as-deposited) denote a thermally oxidized Si substrate, a sapphire substrate, and Mn/Si MLs that were not thermally annealed, respectively. The MLs (as-deposited) were deposited in the following order (from the substrate side): $[\text{Mn}((100-t)/p)/\text{Si}(t/p)]_p$ and $[\text{Mn}(0.6 \times f)/\text{Si}(2.2 \times f)]_{48/f}$ (thickness in nm). To change the Si/Mn composition ratio, the thickness of the Si layer, t , was varied from 50 to 100 nm. To modulate the texture of thin films, period p and thickness factor f were varied from 1 to 16 and from 1 to 6, respectively. The samples annealed at several temperatures between 0-800°C under vacuum of 10^{-6} Pa for 1 hour and in Ar-3% H₂ atmosphere for 10 seconds to 1 hour.

Corresponding Author: Dr. Yosuke Kurosaki, Center for Exploratory Research, Research & Development Group, Hitachi, Ltd., 1-280, Higashi-koigakubo, Kokubunji, Tokyo 185-8601, Japan; E-mail: yosuke.kurosaki.uy@hitachi.com

Citation: Kurosaki Y, Yabuuchi S, Nishide A, Fukatani N, Hayakawa J (2017) Thermoelectric Properties of Texture-controlled MnSi_{1.7}-based Composite Thin Films. Int J Metall Mater Eng 3: 130. doi: <https://doi.org/10.15344/2455-2372/2017/130>

Copyright: © 2017 Kurosaki et al. This is an open-access article distributed under the terms of the Creative Commons Attribution License, which permits unrestricted use, distribution, and reproduction in any medium, provided the original author and source are credited.

The film composition was determined by inductively coupled plasma (ICP) mass spectrometry. The film structure was characterized by X-ray diffraction (XRD) using Cu K_α radiation (RINT1600, Rigaku Corp.), cross-sectional transmission electron microscopy (TEM) (JEM-ARM200F, JEOL Ltd.) with energy-dispersive X-ray spectroscopy (EDX) (HD-2700, Hitachi High-Technologies Corp.), and cross-sectional scanning electron microscopy (SEM) (S-5200, Hitachi High-Technologies Corp.). The in-plane *S* and ρ were measured by 4- and 2-probe methods, respectively (ZEM-3, ADVANCE RIKO, Inc.).

Results and Discussion

Crystal structures and morphology of MnSi_{1.7} thin films fabricated from Mn/Si bi-layers

First, to examine the reaction between Mn and Si in the post-annealing process, the dependence of fabricated materials and their thermoelectric properties on the Si/Mn composition ratio was investigated. Initial Mn/Si multilayers were deposited on Si/SiO_x substrates, in a similar manner to that described in our previous report on MnSi_{1.7} thin films [8]. XRD profiles of a θ - 2θ scan of SiO_x//[Mn(100-*t*)/Si(*t*)]₁ annealed at annealing temperature *T*_a of 800°C in a vacuum are shown in Figure 1 (a). The coexistence of Mn₅Si₃ and MnSi, that of MnSi and MnSi_{1.7}, and that of MnSi_{1.7} and Si were observed when the Si layer thickness *t* was 50, 68, and 80 nm, respectively. The corresponding Si/Mn composition ratio determined by ICP is 0.6, 1.3, and 2.5, respectively. The sequence of material formation from Mn₅Si₃ to Si with increasing the Si/Mn composition ratio corresponds to the Si-Mn binary-phase diagram even when annealing temperature *T*_a was below the melting point of fabricated materials [12]. These results suggest that the observed manganese silicides were obtained by solid-phase reactions, in this case, planar coupling reactions in the interface between Mn and Si layers as observed in previous reports on annealed Mn thin films on Si substrates [9,13]. Since the first nucleated phase in the interface between Mn and Si is known to be Mn₅Si₃ in planar Mn-Si coupling reactions following the rule proposed by Walser and Bené [14], the *T*_a of 800°C is enough high for consuming Mn and Si in the whole film through atomic diffusions. In fact, transition metals are known to be fast diffusers in Si at temperatures above 0.7 *T*_m (the melting point), in this case, 750-850°C [15]. On the other hand, Si single layer with *t* = 100 nm was not crystallized. This result indicates that planar binary coupling reactions support the crystallization of Si. Figure 1 (b) and (c) show dependence of *S* and ρ at room temperature on the Si layer thickness *t*, respectively. The corresponding Si/Mn composition ratio is also shown. Both *S* and ρ rapidly increased when Si/Mn composition ratio exceeded 1.7. This increase originates from formations of semiconducting MnSi_{1.7} and Si, while coexistence with metallic MnSi and/or Mn₅Si₃ is considered to keep the *S* low. As a result, the obtained *S* reached 300 μ V/K when Si became the main phase with MnSi_{1.7} (*t* = 90 nm).

We next investigated the texture of MnSi_{1.7} thin films depending on the fabrication conditions. Figure 2 (a) shows XRD profiles of a θ - 2θ scan of SiO_x//[Mn(27)/Si(73)]₁ annealed at 600-800°C under vacuum. The corresponding Si/Mn ratio of the films was confirmed to be about 1.7 by ICP. Single phase of MnSi_{1.7} was obtained when *T*_a was above 650°C, while MnSi instead of MnSi_{1.7} was observed when *T*_a was above 600°C. The cross-sectional TEM image in Figure 2 (b) shows the existence of large crystallized grains of MnSi_{1.7} phase, which was identified by EDX analysis, in SiO_x//[Mn(27)/Si(73)]₁ annealed at 800°C. As already noted, the first nucleated phase in

planar Mn-Si coupling reactions should be Mn₅Si₃ followed by two reactions involving Si-richer compounds: (Mn₅Si₃ + 2Si \rightarrow 5MnSi) and (4MnSi + 3Si \rightarrow Mn₄Si₇) in the Si rich region as predicted theoretically [14,16,17] and previously observed in annealed Mn thin films on Si substrates [9]. Hence, the observed MnSi phase in thin films annealed at 600°C is considered to be the precursor of MnSi_{1.7} in planar Mn-Si coupling reactions. An SEM image of thin films annealed at 600°C is shown in Figure 3 (a). As shown in this image, the thin film has voids only in the vicinity of the interface between the Mn and Si layers. The fact that both unreacted Mn and Si exist at the bottom and top of the thin film, respectively, indicates that *T*_a of 600°C was not enough for atomic diffusion in the whole area of the thin film. This limited atomic diffusion lead to the formation of not MnSi_{1.7}, which was observed in thin films annealed at above 600°C, but MnSi, which should appear before MnSi_{1.7} formation in planar Mn-Si coupling reactions as depicted in the above reaction formula regarding the formation of manganese silicides.

As for morphology, the thin film annealed at 600°C has even structures except for the interface between the Mn and Si layers. On the other hand, when *T*_a was increased to 800°C, the thin film has markedly depressed structures due to atomic diffusion across the whole thin-film area, as observed in Figure 3 (b). Defects and voids in this structure would degrade the material thermoelectric performance and cause difficulties in practical use.

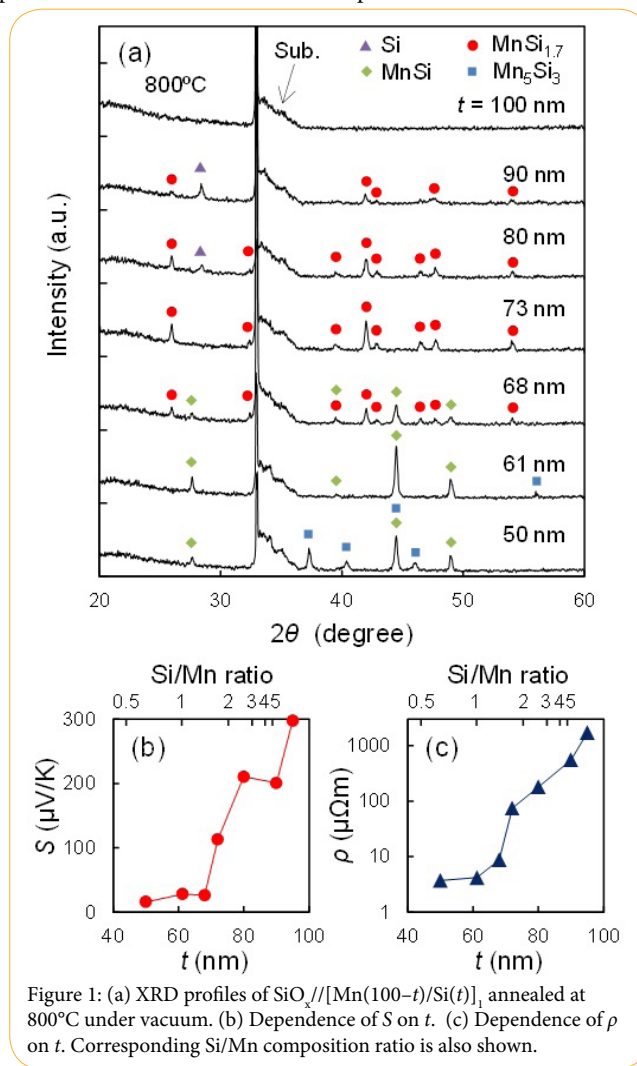


Figure 1: (a) XRD profiles of SiO_x//[Mn(100-*t*)/Si(*t*)]₁ annealed at 800°C under vacuum. (b) Dependence of *S* on *t*. (c) Dependence of ρ on *t*. Corresponding Si/Mn composition ratio is also shown.

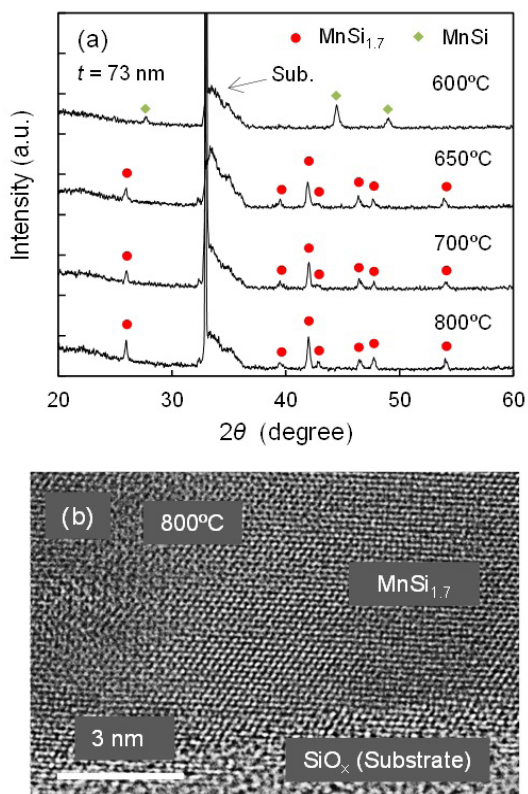


Figure 2: (a) XRD profiles of $\text{SiO}_x//[\text{Mn}(27)/\text{Si}(73)]_1$ annealed at 600-800°C under vacuum. (b) Cross-sectional TEM image of $\text{SiO}_x//[\text{Mn}(27)/\text{Si}(73)]_1$ annealed at 800°C under vacuum.

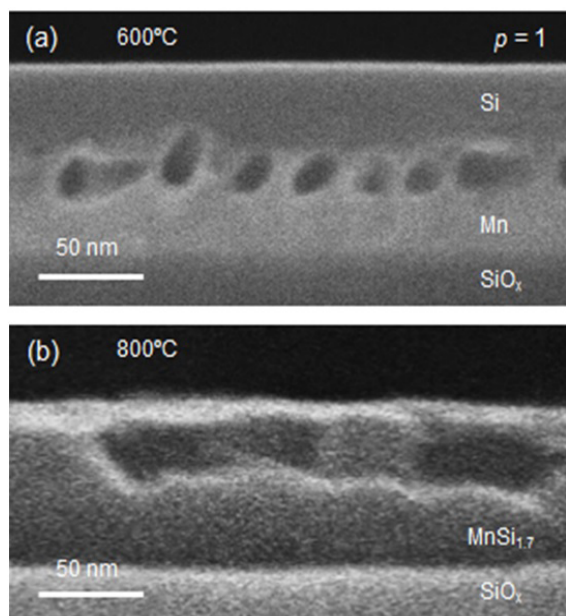


Figure 3: Cross-sectional SEM images of $\text{SiO}_x//[\text{Mn}(27)/\text{Si}(73)]_1$ annealed at (a) 600°C and (b) 800°C. Annealing was performed under vacuum for 1 hour.

Morphology improvements by thinning initial thickness of Mn and Si layers

To obtain smooth and voidless $\text{MnSi}_{1.7}$ thin films, atomic diffusions of Mn and Si should be suppressed by controlling planar Mn-Si

coupling reactions in the interfaces between the initial Mn and Si layers. Since the critical thickness for forming amorphous silicide to cause planar coupling reactions at the interface between transition metal and Si layers is known to be limited to about 2 nm [18], thinning of the initial Mn layers is considered to be effective for improving interfaces would suppress the large voids observed in thin films with a thick initial Mn layer formed by atomic diffusions since atomic diffusions would be prevented after the formation of manganese silicides. Figure 4 shows XRD profiles a θ - 2θ scan of $\text{SiO}_x//[\text{Mn}(27/p)/\text{Si}(73/p)]_p$ ($p = 1, 4, 8, \text{ and } 16$) annealed at 800°C under vacuum for 1 hour. Diffraction peaks of $\text{MnSi}_{1.7}$ are observed, and the peak structures for all films change little. In contrast to the crystal structure, the morphology of the thin films varies significantly depending on p , in other words, the initial thickness of the Mn and Si layers. Figure 5 shows cross-sectional SEM images of $\text{SiO}_x//[\text{Mn}(27/p)/\text{Si}(73/p)]_p$ ($p = 4, 8, \text{ and } 16$) annealed at 800°C under vacuum for 1 hour. The thin films have fewer voids and smooth structures with increasing p , compared with the thin film with $p = 1$ shown in Figure 3 (b). When the thickness of the Mn layer becomes less than 2 nm ($p = 16$), $\text{MnSi}_{1.7}$ single phase with smooth void-free structures was formed. It is considered that this structure is obtained because planar Mn-Si coupling reactions occurred in the whole area of the thin films and diffusion of Mn atoms was limited by thinning the constituent layers.

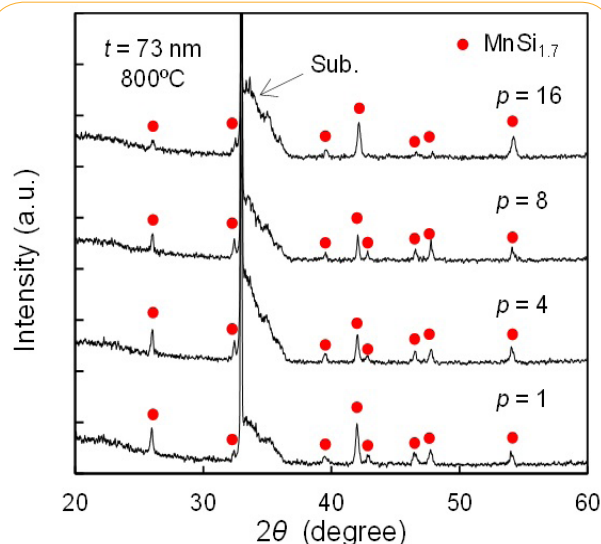


Figure 4: Periodicity dependence of XRD profiles in $\text{SiO}_x//[\text{Mn}(27/p)/\text{Si}(73/p)]_p$ annealed at 800°C under vacuum for 1 hour. ($p = 1, 4, 8, \text{ and } 16$).

Substrate effect on evaluation of Seebeck coefficient

To evaluate the effect of kinds of substrate on S at high temperatures, S of $\text{MnSi}_{1.7}$ thin films on $\text{Si}/\text{SiO}_x(700)$ substrates was measured. In particular, S of the fabricated smooth and homogeneous thin film with $p = 16$ was compared with that of a bare Si substrate, in which the SiO_x layer on the substrate was removed by hydrofluoric acid. Figure 6 shows temperature dependence of S of $\text{SiO}_x//[\text{Mn}(27/16)/\text{Si}(73/16)]_{16}$ annealed at 800°C under vacuum for 1 hour together with that of the bare Si substrate. S of $\text{MnSi}_{1.7}$ thin films on $\text{Si}/\text{SiO}_x(700)$ substrate is almost same as that of $\text{MnSi}_{1.7}$ bulk at room temperature. However, it can be seen from the figure that S of $\text{MnSi}_{1.7}$ thin films rapidly increased at around 300°C followed by the sign inversion at around 350°C. In contrast, S of $\text{MnSi}_{1.7}$ bulk is known to gradually increase with temperature and have a broad maximum at around 400-500°C [2,3]. This anomalous temperature dependence resembles that of the bare Si substrate as shown in Figure 6. Hence, we suspect

that this anomalous temperature dependence is not intrinsic: instead, it reflects the thermoelectric properties of not only the thin films on the substrate but also Si substrate itself which has large S . Similar anomalous temperature dependence in the case of MnSi_{1.7} thin films on a Si/SiO_x(450) substrate has been previously reported [22]. According to the above results regarding S at high temperatures, the thickness of insulating SiO_x layer, 700 nm, is considered to be not enough for evaluating thermoelectric properties especially at high temperatures. Accordingly, sapphire substrates, which are insulating, were used in our study for determining S at high temperatures. In the following sections, after investigating crystal structures of MnSi_{1.7}-based composite thin films with Si on sapphire substrates, S and ρ of MnSi_{1.7} thin films were evaluated.

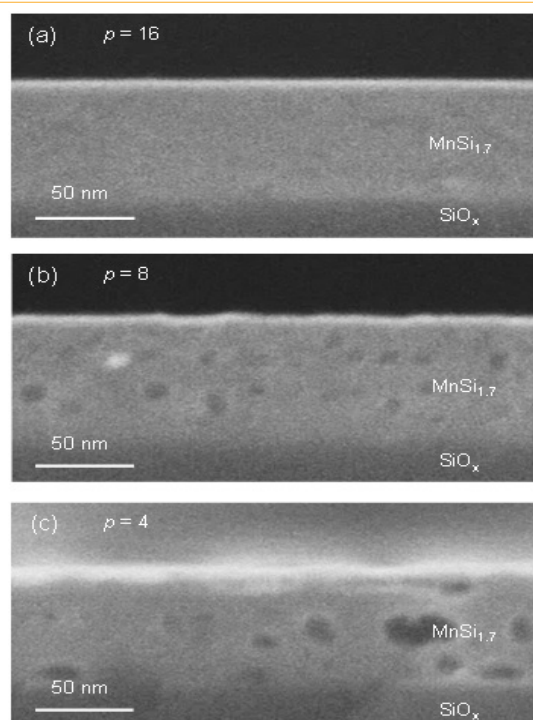


Figure 5: Cross-sectional SEM images of SiO_x//[Mn(27/p)/Si(73/p)]_p annealed at 800°C under vacuum for 1 hour. (p = 4, 8, and 16).

Crystal structures and thermoelectric properties of MnSi_{1.7}-based composite thin films on sapphire substrate

The crystal structures and thermoelectric properties of MnSi_{1.7}-based thin films fabricated on sapphire substrates were investigated as follows. First, we investigated the effect of reducing the initial Mn layer thickness on the crystal structure and also on both S and ρ when the Si/Mn composition ratio exceeded 1.7 and the substrate was sapphire. Figure 7 (a) shows a dependence of XRD profiles of a θ - 2θ scan on the thickness factor f in Sapp//[Mn(0.7 \times f)/Si(2.2 \times f)]_{48/f} annealed at 800°C under vacuum for 1 hour. The Si/Mn composition ratio is 2.1 and hence the coexistence of MnSi_{1.7} and Si is expected if all Mn react with Si. In all films, dif-fraction peaks from MnSi_{1.7} were observed and MnSi_{1.7} was found to be the main phase. On the other hand, the broad diffraction peaks of Si, which were observed when f is 4 or 6, disappear with decreasing f . In the case of $f = 1$, the peaks became sharp and large, indicating the MnSi_{1.7} grain growth and improved MnSi_{1.7} crystallinity. These results indicate that crystallized MnSi_{1.7}-based composite thin films could be obtained by reducing the initial Mn layer thickness on the sapphire substrates. Figure 7 (b) and (c) show dependence of S and ρ at room

temperature on thickness factor f , respectively. The ρ is about 30% small when $f = 1$ compared to the other films, while S stayed almost constant. This small ρ is considered to originate from suppression of grain boundary scatterings owing to the MnSi_{1.7} grain growth as was pointed out above. The improved crystallinity of MnSi_{1.7} as a result of planar Mn-Si coupling reactions occurring across the whole area of the thin films might also contribute. The ρ also gradually increases with f increase from 2 to 6. This increase may be due to the appearance of voids with increasing f as was observed in Figure 5. In fact, the density gradually decreases from 4.2 to 3.9 g/cm³ with f , while that hardly differs if compared between thin films with $f = 1$ and 2 (data are not shown here) [23]. The increase may also reflect suppression of point scatterings due to the shrink in size of remaining Si and/or the fraction decrease of Si resulting from the promotion of coupling reactions by thinning the initial Mn layer thickness.

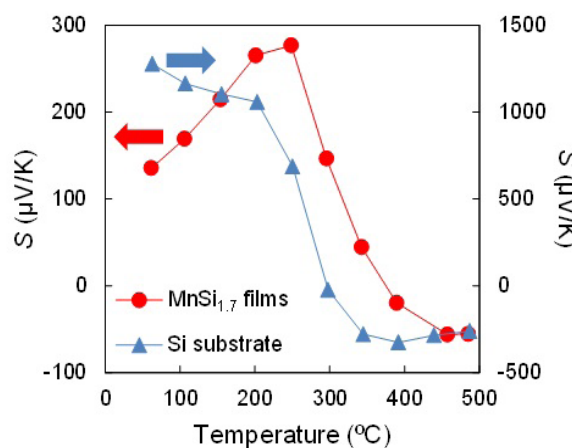


Figure 6: Temperature dependence of S and ρ in SiO_x//[Mn(27/16)/Si(73/16)]₁₆ annealed at 800°C in a vacuum for 1 hour and that of bare Si substrate.

To investigate planar Mn-Si coupling reactions promoting the fabrication of our MnSi_{1.7}-based thin films in detail, effects of annealing conditions on crystal structures and thermoelectric properties of fabricated MnSi_{1.7}-based thin films were evaluated. Figure 8 (a) shows a dependence of XRD profiles of a θ - 2θ scan on T_a for Sapp//[Mn(0.7)/Si(2.2)]₄₈ annealed at 200-800°C under vacuum. The XRD profiles are almost similar and, in the case that T_a was above 400°C, only diffraction peaks from MnSi_{1.7} are observed, while Mn/Si MLs (as-deposited) show no diffraction peak and the diffraction peak from MnSi appears in the case that T_a was 200°C. The amorphous state of Mn/Si MLs (as-deposited) agreed well with previous reports and indicates that planar Mn-Si coupling reactions contribute to the formation of MnSi_{1.7} [9]. The appearance of MnSi phase in thin films annealed at low T_a of 200°C may be due to insufficient reactions as was observed in Figure 3 (a). Figure 8 (b) and (c) show dependences of S and ρ at room temperature on T_a , respectively. Mn/Si MLs (as-deposited) shows S of 15 μ V/K and ρ of 10 μ Ω m. Both the low S and ρ suggest that the Mn/Si MLs (as-deposited) are metallic and semiconducting MnSi_{1.7} was not formed. After Mn/Si MLs (as-deposited) were annealed at 200°C, both S and ρ increased above 150 μ V/K and 250 μ Ω m, respectively, because of the formation of MnSi_{1.7} phase. The increase of ρ with increasing T_a may reflect that the fraction of semiconducting MnSi_{1.7} increases instead of the metallic secondary phase: MnSi and/or remaining Mn. On the other hand, the observed ρ is pretty high compared with that of bulk MnSi_{1.7}, which ranges from 15 to 40 μ Ω m [2,3]. This large value is indicative of remnant of nearly

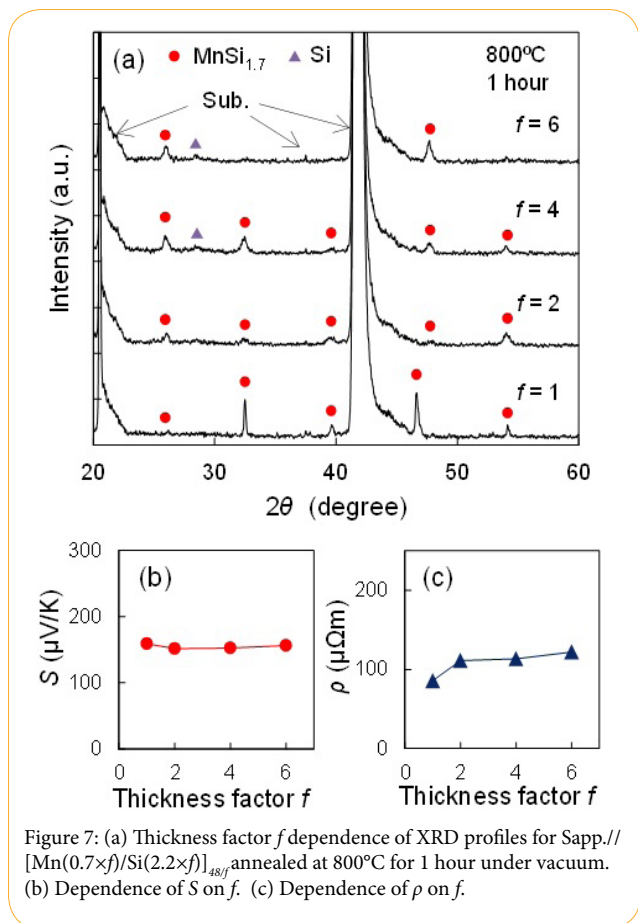


Figure 7: (a) Thickness factor f dependence of XRD profiles for Sapp.//[Mn(0.7 \times f)/Si(2.2 \times f)]_{48f} annealed at 800°C for 1 hour under vacuum. (b) Dependence of S on f . (c) Dependence of ρ on f .

insulating Si because the Si/Mn composition ratio of the film is 2.1 [24]. The ρ significantly decreased to 86 $\mu\Omega\text{m}$ when T_a increased above 600°C. This reduction of ρ is possibly due to the promotion of the coupling reactions towards MnSi_{1.7} resulting in the decrease of the Si fraction. The improvements of crystallinity with increasing T_a and nano-crystallization of Si phase with increasing T_a might also contribute to the reduction of ρ . As discussed in the previous section for SiO_x//[Mn(27)/Si(73)]₁ annealed at 600°C, an inhomogeneous state was easily formed by insufficient atomic diffusions of Mn and Si in the thin films annealed at low T_a .

Note that MnSi_{1.7} phase was obtained even when T_a was 200°C, which is fairly low compared with other previous reports on MnSi_{1.7}-based thin films and bulk [2,3,9]. Absence of Mn₃Si₃, which is known to appear as a first phase through planar Mn-Si coupling reactions in Si-rich thin films [14,16,17], indicate that the effective Si concentration increased in the area where planar Mn-Si coupling reactions occurred due to the thinned initial Mn layers. According to the “effective heat of formation model” (EHF) [25], the heat of formation is given by the ratio between the effective concentration limiting element and the compound concentration-limiting element. By reducing the initial Mn layer thickness, it is possible to increase the effective Si concentration through the formation of intermixing interfaces (as discussed in the previous section). When effective Si concentration in the interfaces increased, MnSi_{1.7} becomes preferably stable in accord with the effective heat of formation diagram for Mn-Si shown in a previous report using EHF [26]. Figure 9 (a) shows a dependence of XRD profiles of a θ -2 θ scan on the annealing time t_a for Sapp.//[Mn(0.7)/Si(2.2)]₄₈ annealed at 800°C in atmosphere of Ar + 3% H₂.

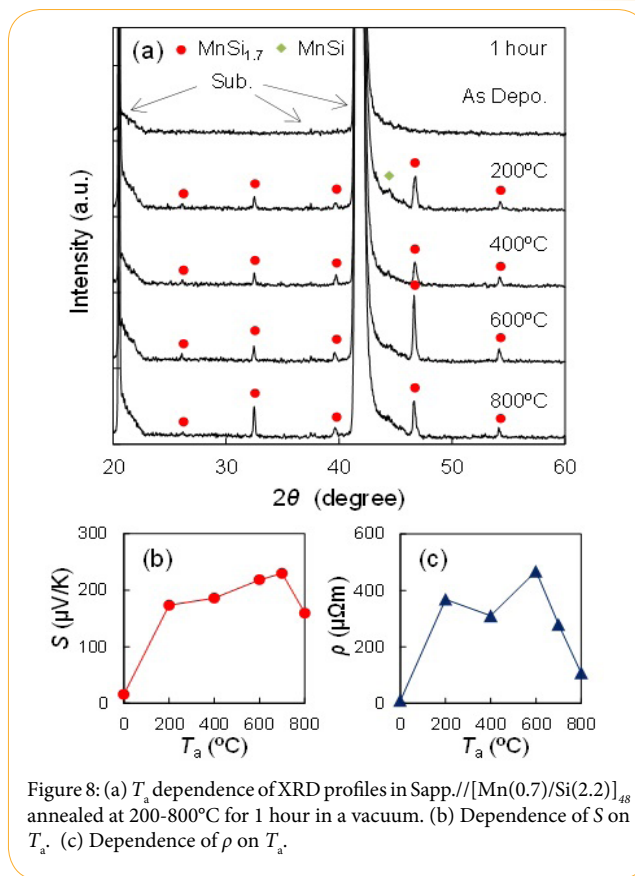


Figure 8: (a) T_a dependence of XRD profiles in Sapp.//[Mn(0.7)/Si(2.2)]₄₈ annealed at 200-800°C for 1 hour in a vacuum. (b) Dependence of S on T_a . (c) Dependence of ρ on T_a .

In the case of all films, diffraction peaks from MnSi_{1.7} were observed and MnSi_{1.7} was found to be the main phase. Since the atomic diffusion strongly depends on both T_a and t_a [15], MnSi should preferably appear when T_a and t_a were decreased, as observed for SiO_x//[Mn(27)/Si(73)]₁ annealed at 600°C. MnSi phase was observed only in thin films annealed for 1 hour and MnSi_{1.7} without coexistence of MnSi even for a short annealing time process also suggests that MnSi_{1.7} becomes energetically stable during silicide formation owing to the thinning of the initial layers. Figure 9 (b) and (c) show dependence of S and ρ at room temperature on t_a , respectively. Clearly, ρ decreased rapidly with increasing t_a and became almost constant when t_a was longer than 1 minute, while S did not change much even when t_a was increased. The decrease of ρ may be due to the homogenization of the fabricated MnSi_{1.7} phase driven by atomic diffusion through the an-nealing process. The nano-crystallization of Si, which could not be identified in this study, caused by annealing from amorphous phase in Mn/Si MLs (as-deposited) might also contribute to the decrease of ρ . Note that the ρ of thin films annealed for 1 hour in atmosphere of Ar + 3% H₂ is about half of that of thin films annealed for 1 hour in a vacuum. The appearance of MnSi phase, which was not observed in thin films annealed in a vacuum, suggest that Mn reacts with Si insufficiently and resultantly metallic MnSi makes the ρ low compared with thin films annealed in a vacuum.

Finally, we evaluated S and ρ of fabricated MnSi_{1.7} thin films at high temperatures because MnSi_{1.7} is known to show the maximum power factor, S^2/ρ , at around 400-500°C [2,3]. Figure 10 (a) and (b) show dependence of S and ρ on temperature for Sapp.//[Mn(0.7)/Si(2.2)]₄₈ annealed at 800°C for 1 hour under vacuum, respectively. Temperature was varied from 50 to 450°C. Annealing temperature T_a and annealing time t_a were fixed to 800°C and 1 hour, respectively, because, according

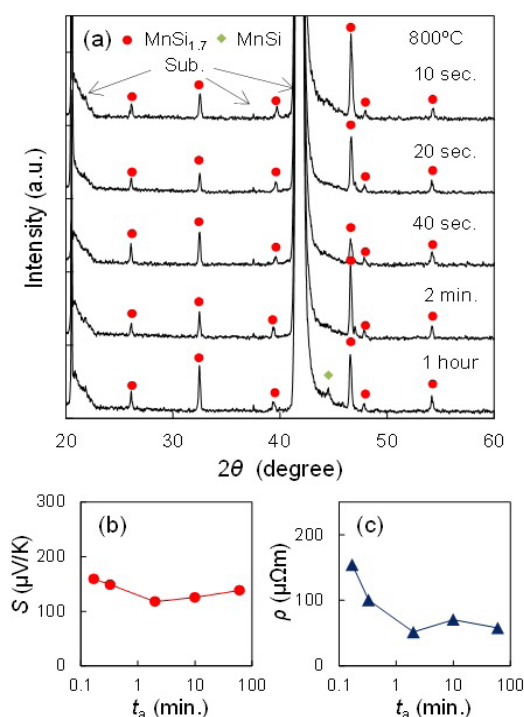


Figure 9: (a) Dependence of XRD profiles for $\text{Sapp.} // [\text{Mn}(0.7)/\text{Si}(2.2)]_{48}$ annealed at 800°C in $\text{Ar} + 3\% \text{H}_2$ atmosphere on annealing time t_a . (b) Dependence of S on t_a . (c) Dependence of ρ on t_a .

to the results in the previous sections, high T_a and long t_a were found to be effective for increasing the power factor. S slightly increased with temperature and reached a maximum around 400°C. Note that this behavior is almost consistent with previous reports on $\text{MnSi}_{1.7}$ bulk [2,3] and clearly different from that of thin films on the $\text{Si}/\text{SiO}_2(700)$ substrates. The difference in S behavior depending on substrates indicates that, for evaluating S and ρ , the insulating substrates should be carefully chosen. Moreover, S reached 225 $\mu\text{V/K}$ at 390°C, which is close to the maximum value of $\text{MnSi}_{1.7}$ -based compounds. On the other hand, ρ decreased with increasing temperature. Since $\text{MnSi}_{1.7}$ is a degenerate semiconductor, ρ was reported to increase with increasing temperature and show a maximum at around 400-500°C [2,3]. This difference from the reported behaviors in temperature dependence may originate from the residual Si in the composite films because the Si/Mn composition ratio of the fabricated thin films is 2.1. Similar temperature dependence of ρ in the case of Si-rich $\text{MnSi}_{1.7}$ thin films has been also previously reported [27]. As for f dependence, S of thin films with $f = 1$ had stronger temperature dependence than those with $f = 2, 4,$ and 6 , while ρ of the thin film with $f = 1$ was much lower than those with $f = 2, 4,$ and 6 . The behavior of S may reflect the improved crystallinity of semiconducting $\text{MnSi}_{1.7}$ with decreasing the initial thickness of the Mn layers (as discussed in the previous section). The reduction of ρ with decreasing f is considered to be due to the suppression of grain boundary scatterings, disappearance of voids, and the suppression of point scatterings of remaining Si as was discussed previously.

Conclusion

Thermoelectric properties of $\text{MnSi}_{1.7}$ -based composite thin films with Si were investigated when the texture of thin films was changed. $\text{MnSi}_{1.7}$ thin films were fabricated by annealing Mn/Si multilayered thin films and initial thickness of the constituent layers was changed

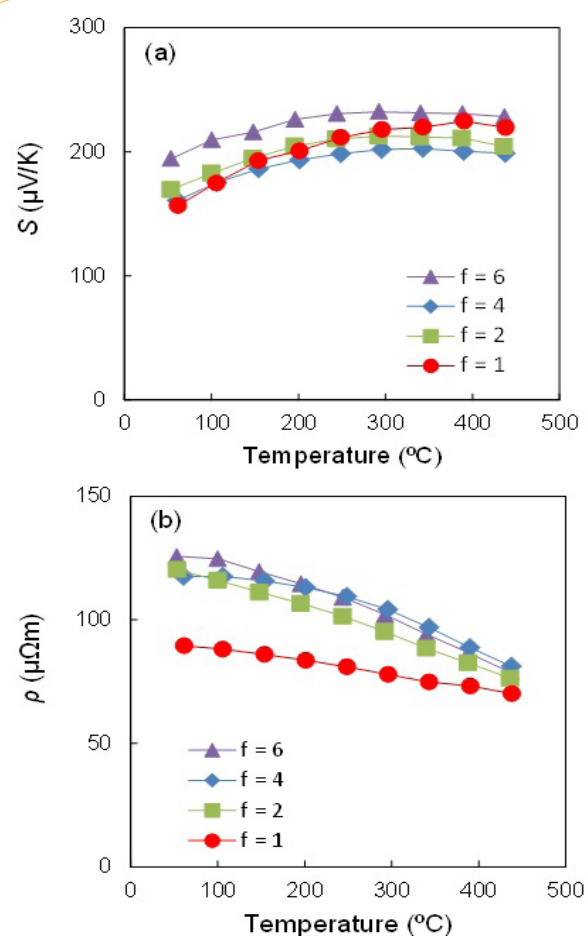


Figure 10: Temperature dependence of thermoelectric properties of $\text{Sapp.} // [\text{Mn}(0.7 \times f)/\text{Si}(2.2 \times f)]_{48/f}$ annealed at 800°C for 1 hour under vacuum. (a) S and (b) ρ

to modulate the texture. By thinning the initial constituent layers, smooth and voidless crystalline $\text{MnSi}_{1.7}$ -based thin films were obtained because planar Mn-Si coupling reactions are considered to occur across the whole area of the thin films. It was found that $\text{MnSi}_{1.7}$ may be the first formed phase by planar Mn-Si coupling reactions in thin films with the initial Mn layer thickness below 2 nm. The effect of annealing temperature and annealing time on crystal structure and thermoelectric properties was also investigated. As a result, ρ was decreased about 30% by reducing initial Mn thickness and large S of 225 $\mu\text{V/K}$ was obtained at 390°C.

Competing Interests

The authors have no competing interests with the work presented in this manuscript.

Author Contributions

All the authors substantially contributed to the study conception, the acquisition of results, and the interpretations as well as drafting the manuscript.

Funding

This paper is based on results obtained from the Future Pioneering Program "Research and Development of Thermal Management and

Technology” commissioned by the New Energy and Industrial Technology Development Organization (NEDO). This work is also supported by TherMAT.

References

1. Yamamoto A, Ghodke S, Miyazaki H, Inukai M, Nishino Y, et al. (2016) Thermoelectric properties of supersaturated Re solid solution of higher manganese silicide. *Jpn J Appl Phys* 55: 020301.
2. Fedorov MI and Zaitsev VK (2006) *Thermoelectric Handbook*. CRC Press Chap. 31.
3. Miyazaki Y (2013) *Thermoelectric Nanomaterials*. Springer Chap. 7.
4. Migas DB, Shaposhnikov VL, Filonov AB, Borisenko VE, Dorozhkin NN (2008) Ab initio study of the band structures of different phases of higher manganese silicides. *Phys Rev B* 77: 075205.
5. Yabuuchi S, Kageshima H, Ono Y, Nagase M, Fujiwara A, Ohta E (2008) Origin of ferromagnetism of MnSi_{1.7} nanoparticles in Si: First-principles calculations. *Phys Rev B* 78: 045307.
6. Venkatasubramanian R, Siivola E, Colpitts T, O'Quinn B (2001) Thin-film thermoelectric devices with high room-temperature figures of merit. *Nature* 413: 597-602.
7. Dresselhaus MS, Chen G, Tang MY, Yang R, Lee H, et al. (2007) New Direction for Low-Dimensional Thermoelectric Materials. *Adv Mater* 19: 1043-1053.
8. Kurosaki Y, Yabuuchi S, Nishide A, Fukatani N, Hayakawa J (2016) Reduction of thermal conductivity in MnSi_{1.7} multi-layered thin films with artificially inserted Si interfaces. *Appl Phys Lett* 109: 1.4960634.
9. Allam A, Boulet P, Record MC (2013) Phase formation in Mn-Si thin films during rapid thermal annealing. *Intermetallics* 37: 69-75.
10. Nedelcu I, E van de Kruijs RW, Yakshin AE, Bijkerk F (2007) Temperature-dependent nanocrystal formation in Mo/Si multilayers. *Phys Rev B* 76: 245404.
11. Streller F, Agarwal R, Mangolini F, Carpick W (2015) Novel metal silicide thin films by design via controlled solid-state diffusion. *Chem Mater* 27: 4247-4253.
12. Massalski TB (1996) *Binary alloys phase diagrams*. ASM: Materials Park.
13. Zhang L, Ivey DG (1991) Low temperature reactions of thin layers of Mn with Si. *J Mater Res* 6: 1518-1531.
14. Walsler RM, Bené RW (1976) First phase nucleation in silicon-transition-metal planar interfaces. *Appl Phys Lett* 28: 624-625.
15. Weber ER (1983) Transition metals in silicon. *Appl Phys A* 30: 1-22.
16. Tsaur BY, Lau SS, Mayer JW, and Nicolet MA (1981) Sequence of phase formation in planar metal-Si reaction couples. *Appl Phys Lett* 38: 922-924.
17. Gösele U and Tu KN (1982) Growth kinetics of planar binary diffusion couples: "Thin-film case" versus "Bulk cases". *J Appl Phys* 53: 3252-3260.
18. Saša B, Stearns DG, and Kearney PA (2001) Investigation of the amorphous-to-crystalline transition in Mo/Si multilayers. *J Appl Phys* 90: 1017-1025.
19. Holloway K, Sinclair R (1988) High-resolution and in situ TEM studies of annealing of Ti-Si multilayers. *J Less-Common Met* 140: 139-148.
20. Windt DL, Christensen FE, Craig WW, Hailey C, Harrison FA, et al. (2000) Growth, structure, and performance of depth-graded W/Si multilayers for hard x-ray optics. *J Appl Phys* 88: 460-470.
21. Yulin S, Feigl T, Kuhlmann T, and Kaiser N (2002) Interlayer transition zones in Mo/Si superlattices. *J Appl Phys* 92: 1216-1220.
22. Hou QR, Zhao W, Chen YB, and He YJ (2010) Preparation of n-type nano-scale MnSi_{1.7} films by addition of iron. *Mat Chem Phys* 121: 103-108.
23. The density of thin films was evaluated by XRR (X-ray Reflectivity) measurements. The density was determined from the total reflection critical angle and estimated to be 4.2, 4.2, 4.0, and 3.9 g/cm³ when f is 1, 2, 4, and 6, respectively.